THE ASSIMILATION ANALYSIS OF 2D SHALLOW WATER FLOW MODEL WITH THE ADJOINT METHOD FOR THE PREDICTION OF DOWNSTREAM WATER LEVELS

Tetsuaki Mikami
Graduate School of Science and Engineering, Chuo University, Kasuga 1-13-27, Bunkyo-ku, Tokyo 112-8551, Japan,
e-mail : a19.trp8@g.chuo-u.ac.jp

Shoji Fukuoka
Research and Development Initiative, Chuo University, Kasuga 1-13-27, Bunkyo-ku, Tokyo 112-8551, Japan,
e-mail : sfuku@tamacc.chuo-u.ac.jp

Akihide Watanabe
TOKEN C. E. E. Consultant Co., Ltd., Kitaootsuka 1-15-6, Toshima-ku, Tokyo 170-0004, Japan,
e-mail : watanabe-ak@tokencon.co.jp

ABSTRACT

Providing accurate water level forecasts is important to ensure the timely evacuation of residents put at risk by a levee overflow or breach. The purpose of this study is to clarify the propagation characteristics of flood flow in Japan's Tone River and to predict several hours ahead the water level downstream. To this end, we developed a real-time assimilation model with two-dimensional planar flow analysis to determine the temporal change in the water level observed over a long section of the river. Based on the hydraulic quantities obtained from the assimilation analysis, the continuity equation is analyzed using the characteristic curve method, and the propagation time of the flood flow to the downstream prediction section is produced. Results show that the water level propagation time is 3 to 5 hours during the rising phase and 2.5 hours at peak. Water levels are then predicted based on the lead time (i.e., propagation time). The predicted water levels are shown to closely approximate the levels, demonstrating the utility of the method for water level prediction.

Keywords: water surface profiles, water level prediction, propagation characteristics of flood flow, assimilation analysis, adjoint method

1. INTRODUCTION

The increasing frequency of heavy rainfall due to climate change has increased the risk of levee overflows. Since overflows can quickly break down earthen levees, residents living near rivers need real-time information on river flow conditions so that they know when to evacuate. At present, many rivers lack a sufficient number of water level observation sites, making it difficult to accurately evaluate and predict temporal changes in the longitudinal water surface profiles along river banks.

In this study, by using high-water stage data obtained from coarsely arranged water gauges, we effectively estimate the temporal change in water surface profiles in Japan's Tone River. The purpose of the study was to clarify the flood flow propagation characteristics and predict water levels in the downstream section from the current time to several hours ahead.

We first developed an assimilation analysis model for the water surface profiles of a 50 km section of the Tone River (long section) by applying the adjoint method to a two-dimensional shallow water flow model (e.g., Sanders et al. 2000, Yoshida 2012, Nishiguchi et al. 2017, Watanabe et al. 2017 and Watanabe et al. 2018). When applied to a September 2013 flood event, the assimilation model closely approximated the temporal changes in water levels observed at 7 sites along the river and simultaneously identified as control variables the flow rate, roughness coefficients, and the permeability coefficients of vegetation. The data assimilation method used in this study has adapted the adjoint method, which has high dynamical consistency and water balance consistency. The inverse estimation of the roughness coefficient has been studied by assimilation analysis using the adjoint method. (e.g., Ding et al. 2000, 2005 and Yoshida et al. 2011).

Next, based on the assimilation analysis results for the long section, the water level for a 17 km downstream section of the river is predicted by applying two-dimensional flow analysis. The forecasting period for this method corresponds to the time of the flood flow propagating to the section targeted for prediction. Using the

cross-sectional averaged quantities of water level, river width, water surface gradient, and roughness coefficients obtained from the assimilation analysis, characteristics of the longitudinal and temporal changes in discharge are examined. The propagation time is then estimated by the continuity equation using the characteristic curve method. Our intent is to establish a way to predict water levels up to several hours ahead based on this analysis method using the longitudinal propagation characteristics of the water level. And also, in order to confirm the practicality of this analysis method as a real-time flood forecasting, we will show the time required for the analysis and how often the predicted water level information is provided to residents.

2. DESCRIPTION OF THE ADJOINT MODEL

The cost function for this adjoint method can be expressed as

$$\begin{aligned} & J_T\left(Q_{bound}, n, K\right) \\ & = J_H + J_Q + J_{n\_init} + J_{K\_init} \\ & = \int_{Ta}^{T}\iint_{A}\sum_{mH}\sum_{k}\delta\left(x-x_{mH}, y-y_{mH}, t-t_k\right)\frac{\left\{H_c\left(x,y,t\right)-H_o\left(x,y,t\right)\right\}^2}{2\sigma_{Ho}^2}dAdt \\ & + \int_{Ta}^{T}\iint_{A}\sum_{mQ}\sum_{k}\delta\left(x-x_{mQ}, t-t_k\right)\frac{\left\{Q_c\left(x,t\right)-Q_o\left(x,t\right)\right\}^2}{2\sigma_{Qo}^2}dAdt \\ & + \sum_{id=1}^{num\_an}\frac{\left\{n\left(id\right)-n_{init}\left(id\right)\right\}^2}{2\sigma_{n\_init(id)}^2} + \sum_{id=1}^{num\_ak}\frac{\left\{K\left(id\right)-K_{init}\left(id\right)\right\}^2}{2\sigma_{K\_init(id)}^2} \end{aligned} \tag{1}$$

Here, J_T is the total cost to be minimized and is a function of three uncertain control variables. Variable Q_{bound} is the discharge at the upstream end, n is Manning's roughness coefficient for beds, and K is the permeability constant for tree communities.

Terms J_H and J_Q on the right-hand side of the equation are the total misfit for the water level and the discharge, respectively. J_{n_init} and J_{K_init} are the sum of the squared differences between the values obtained from the assimilation analysis and the initially assumed (standard) values of n and K, respectively. The values for n and K were constrained in some ranges to avoid any locally abnormal values. Among the four terms, the most influential is the first regarding errors in water level. The meanings of the other parameters are as follows: Ta and T are the initial and last time of calculation, respectively; (x_{mH}, y_{mH}) are the coordinates of the location of the water gauge; t_k is the observation time; x_{mQ} is the location of the discharge observation station; H_0 and Q_0 are the observed water level and discharge, respectively; H_c and Q_c are calculated water level and discharge, respectively; σ_{H0} and σ_{Q0} are the standard deviation of the error of the observed water level and the discharge, respectively; A is the area of the horizontal plane; num_an and num_ak are numbers representing the classifications of Manning's bed surface roughness and the permeability coefficient, respectively; n_{init} and K_{init} are the initial values of n and K, respectively, in the assimilation analysis; and σ_{n_init} and σ_{K_init} are the standard deviations of n and K, respectively.

The continuity equation is written as $F_h(U, V, h) = 0$, where U and V are longitudinal and transverse velocity, respectively, and h is water depth. Then, the longitudinal and transverse momentum equations are written as $F_U(U, V, h) = 0$ and $F_V(U, V, h) = 0$, respectively. Finally, the functional to be minimized in the Lagrange multiplier method under the constraint of the shallow water equations is written as follows:

$$J = J_T + \int_{T_a}^{T}\int_{A}(\lambda_h \cdot F_h + \lambda_U \cdot F_U + \lambda_V \cdot F_V)dAdt \tag{2}$$

The adjoint matrix that the Lagrange multipliers satisfy was obtained by taking the variation of U, V, and h according to Eq. (2). The gradient vectors for the control variables obtained by differentiating Eq. (2) were solved using a quasi-Newton method. The iteration process is summarized in Figure 1. The steps in the process are described in more detail below.

(a) The unsteady shallow water equations are solved with initial values of Q_{bound}, n, and K to obtain $U(x, y; t+\Delta t)$, $V(x, y; t+\Delta t)$, and $h(x, y; t+\Delta t)$ over the entire calculation area for the next calculation time step.

(b) Misfits are evaluated using Eq. (1).

(c) Lagrange multipliers are calculated from the adjoint matrix.

(d) The functional L is calculated from Eq. (2) and gradient vectors of L relative to Q_{bound}, n, and K are estimated. If convergence is achieved, the process ends.

(e) The variables Q_{bound}, n, and K are updated using a quasi-Newton method if L did not converge. Then, the process returns to step (a) for the next iteration.

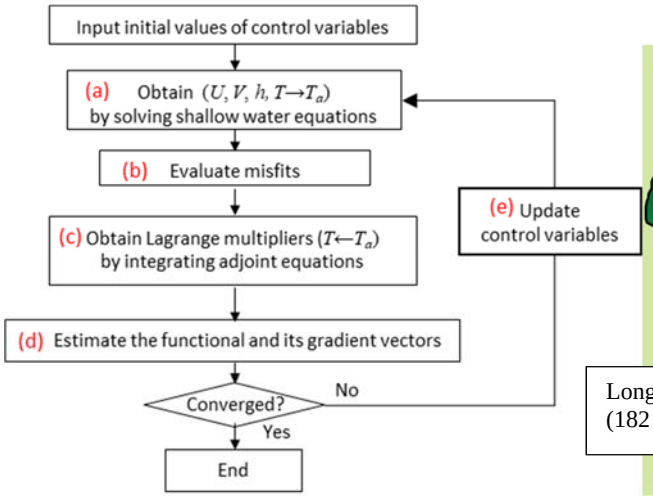

Figure 1. Procedure for assimilation analysis

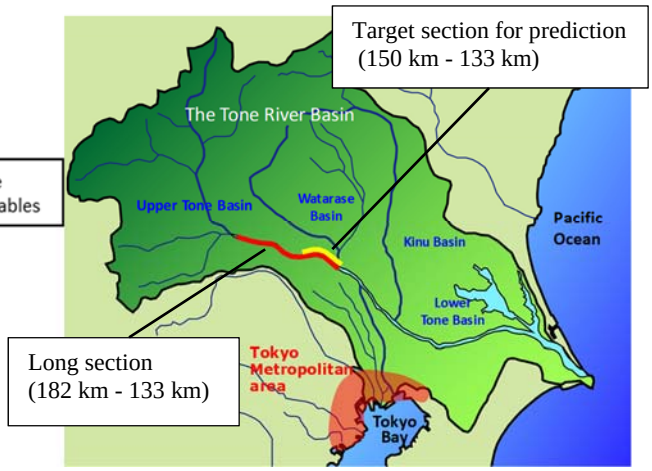

Figure 2. Location of study field in the Tone River watershed

3. ASSIMILATION ANALYSIS FOR THE WATER SURFACE PROFILES DURING THE SEPTEMBER 2013 FLOOD IN THE TONE RIVER

3.1 The study field in the Tone river

Figure 2 shows the location of the study field. The Tone River has its source in the central mountains of Honshu Island, Japan, and flows across the alluvial plain on the north side of Tokyo, eventually discharging into the Pacific Ocean. The model was applied to the flood event observed in September 2013 over a 50 km reach from 182 km to 133 km (long section), where water gauges are installed at 7 points. Based on the assimilation analysis results for the long section, the water level for the 17 km downstream section extending from 150 km to 133 km (target section) was predicted using two-dimensional flow analysis.

Figure 3 is an enlarged view of the channel showing the locations of the water gauges (red triangles). The river channel has a composite cross section with a high-water channel width of approximately 800 m. The low-water channel has an average width and depth of 400 m and 6 m, respectively. Most of the floodplain is covered by grass, but some reed colonies and tree communities remain along the banks of the low-water channel, as indicated in the figure. Channel bed elevations were taken from aerial laser profiling data obtained in 2013; the channel cross-sectional measurement data were obtained in 2012. Vegetation was identified from river environmental information maps prepared in 2011.

The reasons why planar two-dimensional analysis method adopted to the flood flow analysis is as follows. The Tone River is a meandering channel with compound cross-sections (Figure 2 and 3). The flow velocity distribution and fluid resistance is influenced by bed material, ground cover conditions and planar topographical shape of the river. The planar two-dimensional flow analysis can generally consider the above effects except for the flow around the river structure.

Manning's roughness n for each ground cover classification were determined based on report (2003). For the permeability constants of the tree communities K, we adopted the values recommended by Fukuoka et al. (2006 and 2007). These parameter values are listed in Table 1. The time increment for unsteady flow calculation was set to 0.5 seconds in real time.

3.2 Results of the assimilation analysis

Figure 4 (a) shows that the ratio of the cost function to its initial value in the assimilation analysis for the water level observed over two days during the flood period converges as the iteration steps proceed. The ratio decreased sharply through the first 5 iteration steps and became almost constant after the 10th iteration step. Figure 4 (b) shows the convergence process of the values of n and K, which indicate the resistance characteristics of each ground cover classification. All values became stable by the tenth iteration step.

Figure 5 compares the observed discharge and the discharge hydrographs identified by the assimilation analysis. As described below, since the water level in the assimilation analysis agrees with the time change of the observed water levels at stations 1 to 7, the identified discharge hydrographs are smaller than the observed discharge.

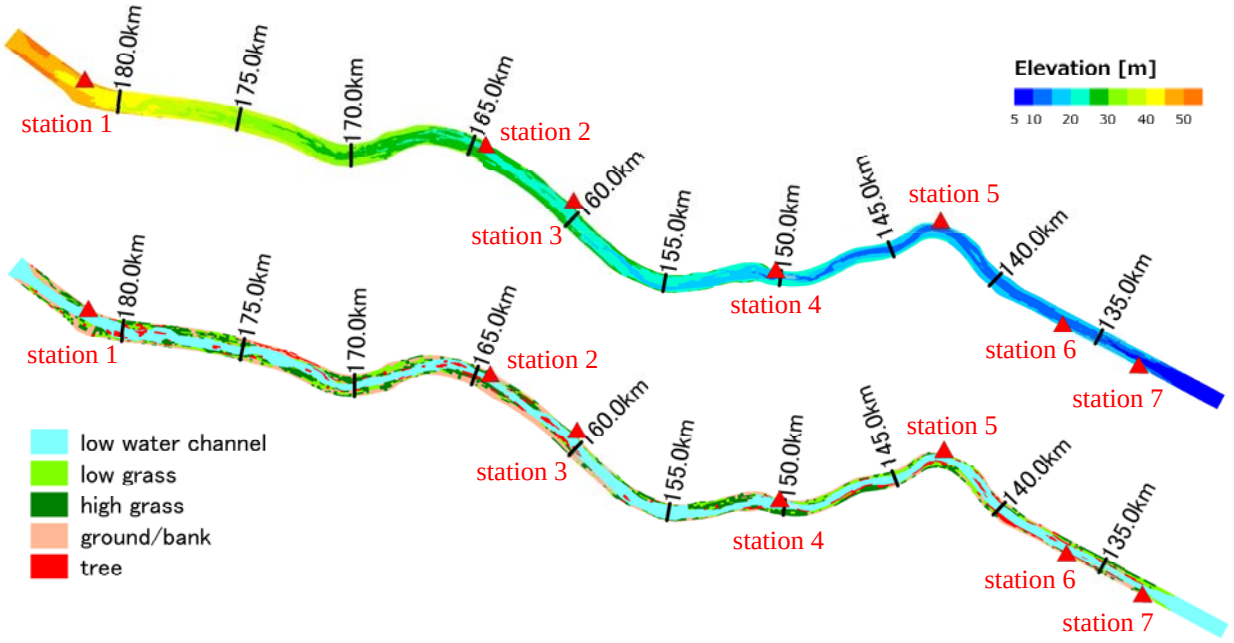

Figure 3. Topography and ground cover of study field

Table 1. Standard values of Manning's roughness and permeability coefficients

Classification	Unit	Pre-set value	Minimum value	Maximum value	Standard deviation
Low-water channel (182km – 169.5 km)	$m^{-1/3}s$	0.032	0.030	0.035	0.0032
Low-water channel (169.5 km – 162 km)		0.030	0.025	0.032	0.0030
Low-water channel (162 km – 154 km)		0.027	0.020	0.030	0.0027
Low-water channel (154 km – 143 km)		0.027	0.020	0.030	0.0027
Low-water channel (143 km – 133 km)		0.025	0.018	0.030	0.0025
Low grass		0.035	0.025	0.050	0.0035
High grass		0.050	0.030	0.080	0.0050
Plain ground or levee		0.025	Fixed Value		
Ground surface of wooded area		0.035	Fixed Value		
Tree communities (permeability constant)	m/s	40	20	80	8

Figure 6 shows a comparison of the computed and observed water level hydrographs. The curves in Figure 7 are the cross-sectional averaged longitudinal water surface profiles of the assimilation analysis during the rising (black), falling (blue), and peak at Station 4 (red). The triangles indicate the observed values at the water gauge stations corresponding to the three lines. As shown, the assimilated water levels are in good agreement with the observed values throughout the flood period.

We consider the reason why the discharge by the assimilation analysis was evaluated smaller than the observed discharge around the peak time in Figure 5. Roughness coefficient changes during the flood due to generation of sand waves and flattening of vegetation, but in this analysis, the roughness coefficient is assumed to be constant through the flood period. The number of water level observation points in the target flood is not enough to examine the time variation of the roughness coefficients. Therefore, the temporal change in the roughness coefficients with the temporal change in the water level is not evaluated in this assimilation analysis, but only the temporal change in the flow rate is estimated. In addition, the preset values of the Manning's roughness coefficients and vegetation permeability coefficients shown in Table 3 are confirmed to be past observations, but the appropriate weights for each term (i.e. J_H, J_Q, J_{n_init}, J_{K_init}) in the cost function (1) due to the variance used are unknown. In this analysis we give 1.0 for all values of weights.

From the above, it can be seen that the water levels obtained from the assimilation analysis closely approximate the observed temporal water levels at 7 points. Furthermore, the flow rate, roughness coefficients, and permeability coefficients of the trees are simultaneously estimated.

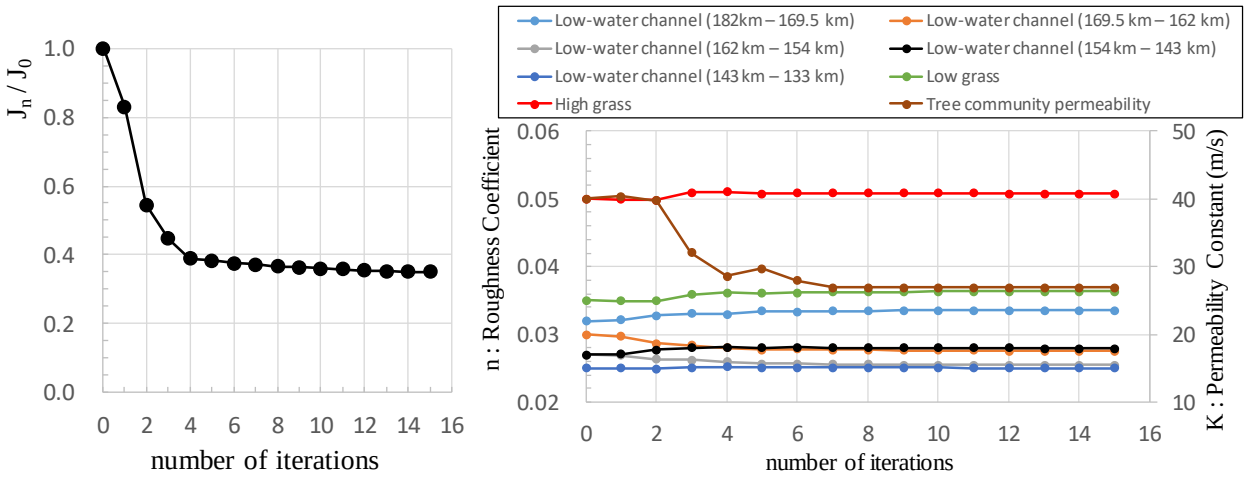

(a) Relative values of cost function (b) Values of *n* and *K*

Figure 4. Convergence process in the assimilation analysis

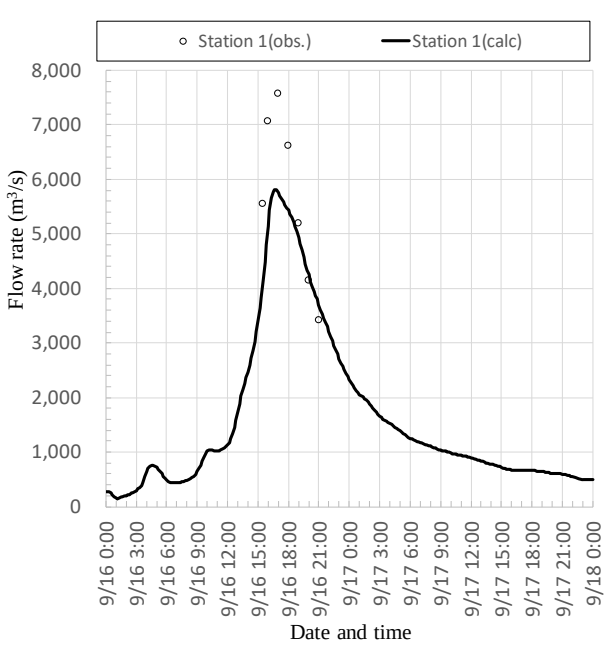

Figure 5. Comparison of the computed and observed discharge hydrographs

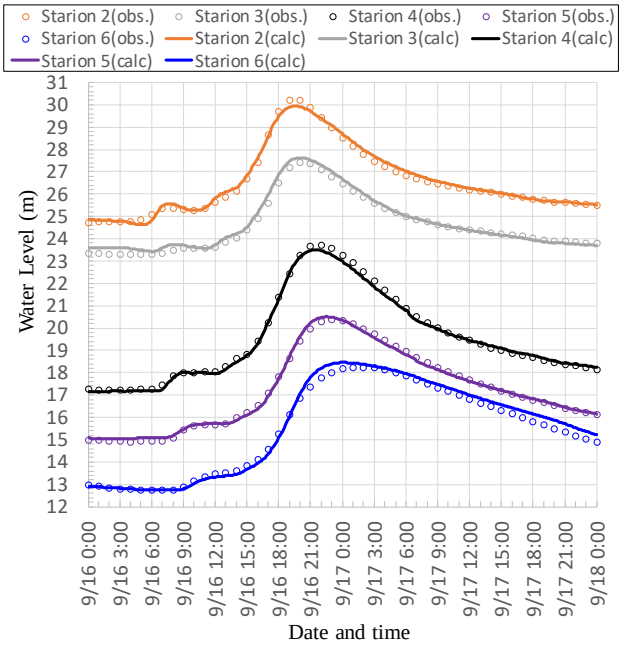

Figure 6. Comparison of the computed and observed water level hydrographs

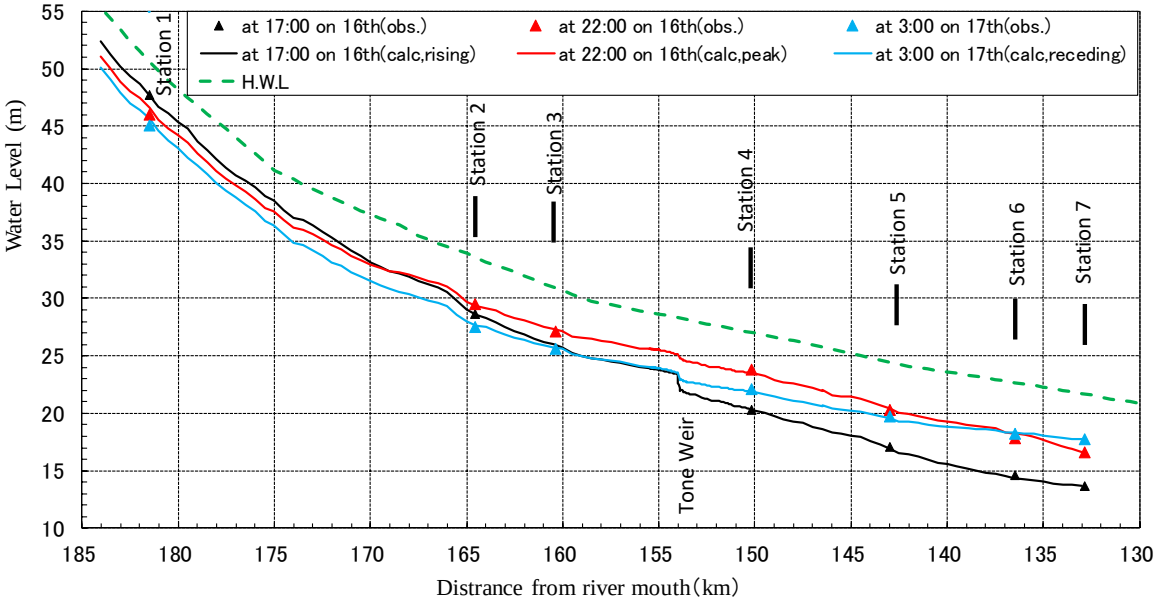

Figure 7. Longitudinal water surface profiles in rising and receding phases and highest water level profile

4. PROPAGATION CHARACTERISTICS AND WATER LEVEL PREDICTION

Based on the results of the assimilation analysis, the propagation characteristics of the flood flow in the Tone River were established, after which the propagation time to the upstream edge of the predicted section for the September 2013 flood was determined. Water level predictions up to the lead time were then calculated. The validity of the approach is confirmed by comparing the predicted water level to the observed level.

4.1 Propagation characteristics of flood flow

Figure 8 shows the cross-sectional average hydraulic quantities obtained from the assimilation analysis up to the upstream edge of the prediction section. These include water level (H), water surface gradient (I_w), discharge (Q) and conveyance (C_o). Here, conveyance (C_o) is defined as

$$C_o = \frac{1}{n} A_c R^{2/3} \quad \text{(e.g., Chow 1959 and Motonaga et al. 2012)}$$

$$Q = C_o I_w^{1/2}$$

where A_c is the cross-sectional area and R is the hydraulic radius.

In this study, the amount obtained from the water level is redefined as the conveyance (C_H).

$$Q = \text{function}[\, A_c(H), R(H), I_w(H), \alpha \,] = \alpha A_c R^{2/3} I_w^{1/2} = \alpha C_H \tag{3}$$

From Figure 8 (a), it can be seen that the relationship between water level and discharge loops downstream (150 km) since the riverbed gradient is smaller there than upstream (180 km). Figure 8 (b) shows that the water surface gradient differs in the rising and receding phases of the flood and that the change in the water surface gradient during the flood period is larger downstream than upstream. Figure 8 (c) shows that the relationship between the flow rate and the water flow capacity is nearly linear.

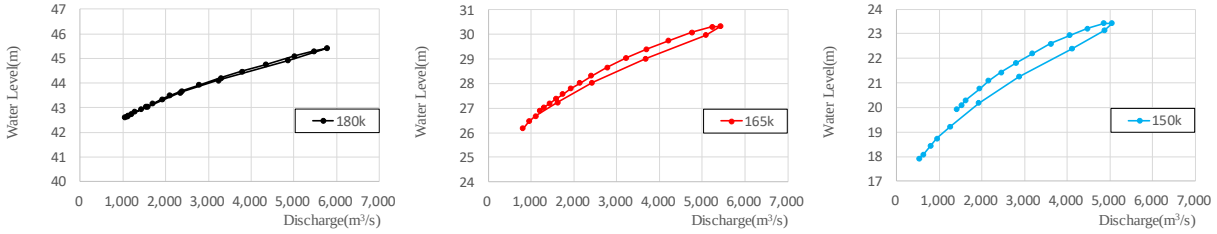

(a) Relationship between discharge and water level

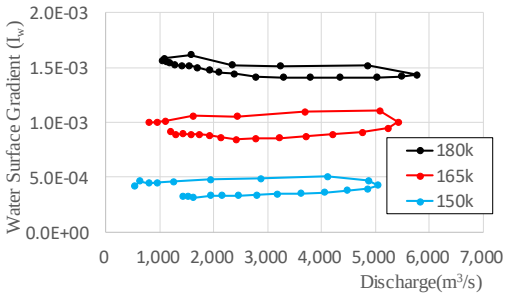

(b) Relationship between discharge and water surface gradient

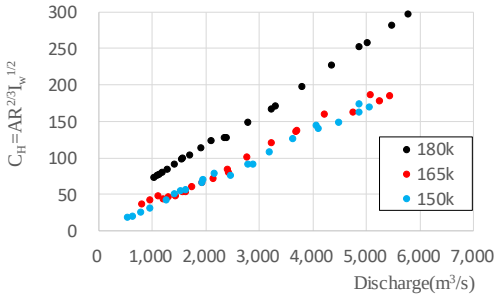

(c) Relationship between discharge and conveyance

Figure 8. Characteristics of flood flow obtained from assimilation analysis

Based on the above results, we can examine the propagation characteristics of the water level. For the continuity equation, it is assumed that the longitudinal change in the discharge can be expressed by the longitudinal change in water level, river width, water surface gradient, and total roughness. This is expressed as follows:

$$\frac{\partial A}{\partial t} + \frac{\partial Q}{\partial x} = \frac{\partial A}{\partial t} + \left(\frac{5}{3}V\right)\frac{\partial A}{\partial x} + \left(-\frac{2}{3}\frac{Q}{B}\right)\frac{\partial B}{\partial x} + \left(\frac{1}{2}\frac{Q}{I_w}\right)\frac{\partial I_w}{\partial x} + \left(\frac{Q}{\alpha}\right)\frac{\partial \alpha}{\partial x} = 0$$

$$\frac{\partial A}{\partial t} + C\frac{\partial A}{\partial x} = -D \tag{4}$$

$$C = \frac{5}{3}V, \quad D = \left(-\frac{2}{3}\frac{Q}{B}\right)\frac{\partial B}{\partial x} + \left(\frac{1}{2}\frac{Q}{I_w}\right)\frac{\partial I_w}{\partial x} + \left(\frac{Q}{\alpha}\right)\frac{\partial \alpha}{\partial x}$$

The propagation distance and time of the water surface profile can be obtained by tracking equation (4) using the characteristic curve method. In this case, C (t, x) and D (t, x) are given as the average values in the cross section obtained from the assimilation analysis results at each time and each place.

As shown in Figure 9 (a), the assimilated water level and the water level given by the characteristic curve method closely agree. Figure 9 (b) shows the path diagram of the characteristic curve. Since equation (4) is

not applicable to the Tone Weir, the calculation is performed separately for the section from the upstream edge to the weir and the section downstream from the weir. From this result, it can be seen that the propagation speed is large during the flood's rising phase (until 17:00 on Sept. 16) but becomes gradually smaller in the receding phase. It can also be seen that the propagation speed changes around the Tone Weir.

Figure 9 (c) shows the propagation time required to reach the upstream edge (150 km: Station 4) of the water level prediction section. The propagation time is 3 to 5 hours during the rising phase and about 2.5 hours at the peak. These propagation times represent predictable lead times that do not require a rainfall intensity distribution, water level, or discharge hydrograph several hours ahead to predict the water level in the section downstream of 150 km.

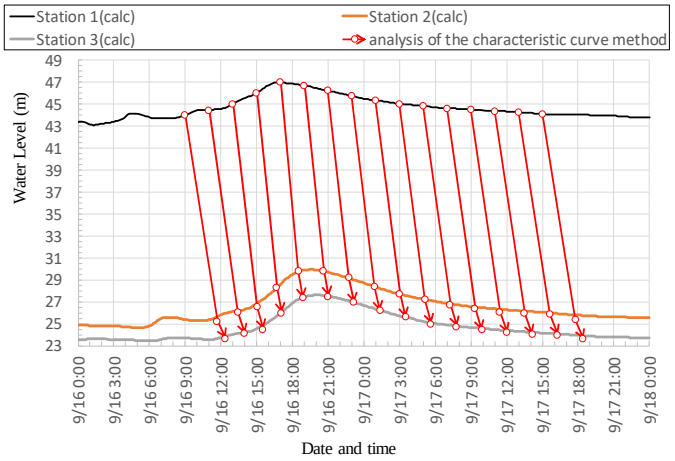

(a) Comparison of the characteristic method and assimilation analysis for water level

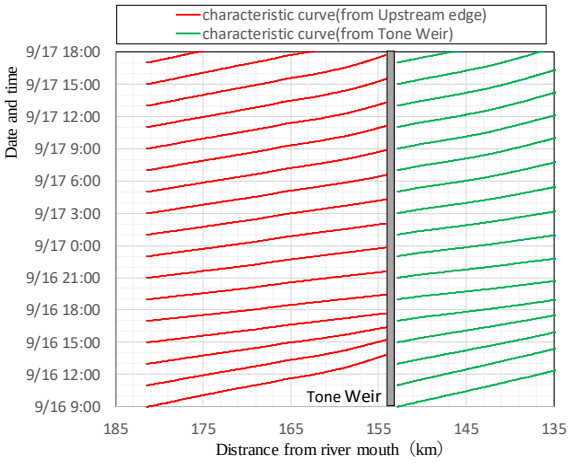

(b) Path diagram of water level propagation

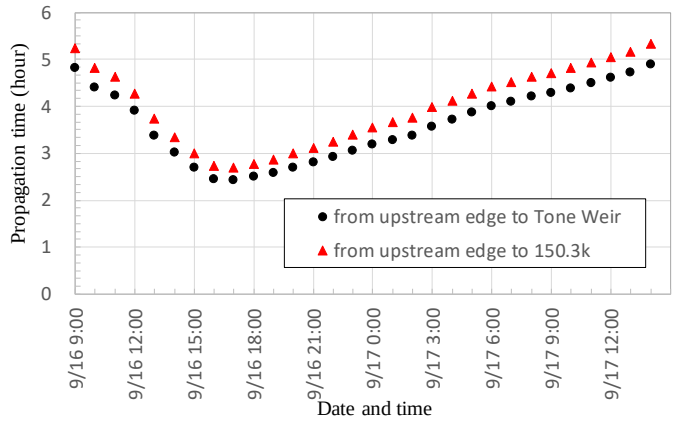

(c) Propagation time of water level

Figure 9. Propagation characteristics of flood flow obtained from assimilation analysis

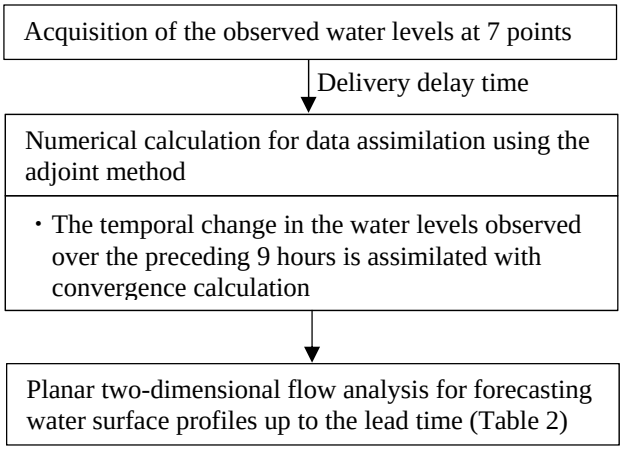

Figure 10. Procedure of analysis method to the ongoing flood

4.2 Water level prediction in the downstream section based on propagation characteristics

Establishing the propagation time of the flood flow up to 150 km (as described above) enables us to conduct our water level prediction analysis for the downstream section. Table 2 shows the forecast start time and the lead time for the analysis. For each of the times indicated in the table, the temporal change in the water level observed over the preceding 9 hours at 7 points in the long section of the river (182 km – 133 km) is assimilated using the adjoint method. The temporal change in the longitudinal water surface profile is then predicted up to the lead time for the target section (150 km – 133 km) using planar two-dimensional flow analysis.

Figure 11 shows a comparison of the predicted and observed water levels at stations 4 and 5. As can be seen in the figure, the predicted water level agrees well with the observed water level until the peak time, although it is slightly higher than the observed water level in the receding phase of the flood. Since the water level at peak is what matters for practical use, the results here affirm the efficacy of the approach.

The analysis method to the ongoing flood evacuation warning for residents is shown in Figure 10 and the applicability of the method is confirmed as follows. The acquisition time of the observed water level (delay time) and the time required for numerical calculation for data assimilation are about 3 minutes and about 1 hour, respectively. The calculation time to estimate the water surface profiles along the embankment from 3 to 5 hours ahead is about 3 minutes. As a result, the total time is within 1.5 hours. These calculations are executed with 6 MPI processes on IBM Power8 (18core, 3.45GHz, 2CPUs).

Table 2 Time to start forecast and lead time for the water level prediction analysis

Time to start forecast (September 2013)	Lead time (hour)
at 9:00 on 16th	5.2
at 15:00 on 16th	3.0
at 18:00 on 16th	2.8
at 21:00 on 16th	3.1
at 0:00 on 17th	3.6

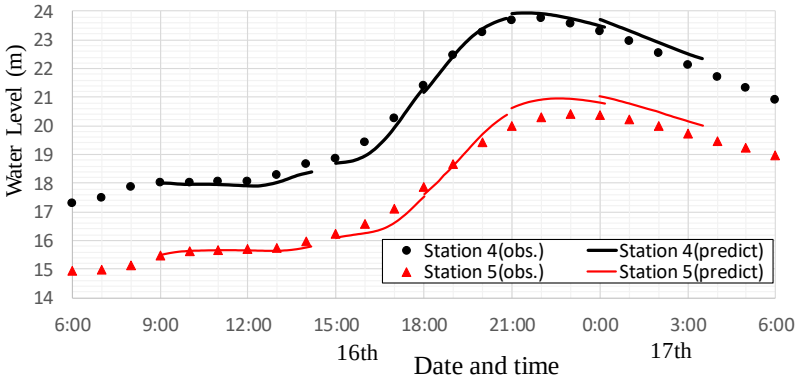

Figure 11. Comparison of the predicted and observed water level

5. CONCLUSION

The study produced several important findings that show the significance and usefulness of the method:

1. The assimilation analysis model accurately reproduced the temporal changes in the water surface profile observed for a 50 km reach of the Tone River during the September 2013 flood.
2. The propagation characteristics of the flood flow and the lead time (propagation time) that are required to predict the water level in the downstream section were quantitatively determined.
3. The predicted water level up to the lead time approximately agrees with the observed water level. Moreover, if this analysis method is used as a flood forecasting system, it is possible to provide the residents with predicted water level information 3-5 hours ahead every 1.5 hours. Therefore, the applicability of water level prediction method for disaster prevention is considered to be high.

REFERENCES

Chow, V.T. (1959), Open-Channel Hydraulics, McGraw-Hill Book Company, pp.128-129

Ding, Y., Jia Y. and Wang, S.S.Y. (2000), Identification of Manning's roughness coefficients in shallow water flows, J. Hydr. Eng., ASCE,Vol.130, No.6, pp.501-510.

Ding, Y. and Wang, S.S.Y. (2005), Identification of Manning's roughness coefficients in channel network using adjoint equation, Int. J. Comput. Fluid Dynam., Vo.19, No.1, pp.3-13.

Fukuoka, S., Shimatani, Y., Tamura, H., Tomari, K., Nakayama, M., Takase, T. and Iuchi, T. (2003), Field experiments on reed deformation and falling and roughness coefficient on floodchannel by flows, Advances in River Engineering, JSCE, 9, 49–54, in Japanese

Fukuoka, S. (2006), River's maintenance and management based on observed water surface profiles of flood flow, Advances in River Engineering, JSCE, 12, 1-6, in Japanese

Fukuoka, S., Fujisawa, H. and Ohnuma, F. (2007), Vegetation permeability coefficient and manning roughness coefficient of the tone river, Advances in River Engineering, JSCE, 13, 333–338, in Japanese

Motonaga, Y., Qian, C., Yamada, T. and Yamasaka, M.(2012), The new type discharge rating method using water level – conveyance curve (hk curve) , Journal of Japan Society of Civil Engineers, Ser. B1(Hydraulic Engineering), Vol.68, No.4, pp.I_1357-I_1362, in Japanese

Nishiguchi, R. and Dan, T. (2017) Real-time water level prediction using adjoint sensitivity analysis, Advances in River Engineering, JSCE, 23, 275-280, in Japanese

Sanders, B. F. and Katopodes, N. D. (2000), Adjoint sensitivity analysis for shallow-water wave control, Journal of Engineering Mechanics, 126-9, pp.909-919.

Watanabe, A., Mikami, T., Kojima, T., Matsunobu, K. and Suzuta, H. (2017), Study on the data assimilation of the water surface profiles using 2d shallow water flow model and adjoint method, Advances in River Engineering, JSCE, 23, 197–202, in Japanese

Watanabe, A., Matsunobu, K., Mikami, T., Kojima, T. and Suzuta, H. (2018), Study on the density of observation data necessary for the hydraulic numerical analysis and the data assimilation, Journal of Japan Society of Civil Engineers, Ser. B1(Hydraulic Engineering), Vol.74, No.5, pp.I_613-I_618, in Japanese

Yoshida, K. and Ishikawa, T. (2012), Inverse estimation of river discharge hydrograph in open-channels with flood plains by using adjoint shallow-water model, Journal of Japan Society of Civil Engineers, Ser. B1(Hydraulic Engineering), Vol.68, No.4, pp.I_1261-I_1266, in Japanese

Yoshida, K. (2011), Inverse estimation of time-series variation of bed roughness coefficients by using adjoint shallow-water model, Journal of Japan Society of Civil Engineers, Ser. A2(Journal of applied mechanics), Vol.14, No.2, pp.I_533-I_540, in Japanese